Engineering Solid Mechanics 11 (2023) 11-22

Contents lists available at GrowingScience

Engineering Solid Mechanics

homepage: www.GrowingScience.com/esm

Optimization and finite element modeling of orthogonal turning of Ti6Al4V alloys: A comparative study of different optimization techniques

C.S. Sumesh[a] and Ajith Ramesh[a*]

[a]*Department of Mechanical Engineering, Amrita School of Engineering, Coimbatore, Amrita Vishwa Vidyapeetham, India*

ARTICLEINFO

Article history:
Received 25 August 2022
Accepted 1 November 2022
Available online
1 November 2022

Keywords:
Ti6Al4V
Orthogonal Turning
Finite Element Model
RSM
Taguchi
TLBO

ABSTRACT

The main goal of this research is to compare the various optimization strategies (Response Surface Methodology, Taguchi, and Teaching Learning Based Optimization) for orthogonal turning of Hard to Machine materials. The workpiece material in this work is Ti6Al4V alloys. After selecting cutting speeds in the High-Speed Machining range, orthogonal turning tests are performed on the material for a specific combination of machining parameters – Depth of Cut, Cutting Speed, and, Feed Rate. A Lathe Tool Dynamometer is used to record the cutting forces from the trials. After combining Johnson Cook Material and Damage models, a comprehensive Finite Element Model is created to model the Orthogonal Turning of Ti6Al4V alloys. Experiments conducted previously validate the developed model. Three different strategies, namely RSM, Taguchi, and TLBO, were used to optimise machining parameters for minimal Cutting Force. The approaches are compared for the best combination of machining parameters and the best Cutting Force value. Analysis of Variance is used to study the impact of machining factors on Cutting Force.

1. Introduction

Ti-6Al-4V is the most often used titanium alloy in aerospace applications because of its excellent corrosion resistance, high strength-to-weight ratio, and fatigue capabilities at high temperatures (Olvera et al., 2012; Sahu et al., 2018; Bandapalli et al., 2018; Jamil et al., 2019; Gao & Zhang, 2013; Pervaiz et al., 2014; Wu & Guo, 2014; Choudhary & Paul, 2019). Ti6Al4V, on the other hand, is difficult to machine because of the significant chemical reactivity of titanium with the tool material favours diffusion wear and strong bonding at the rake face, resulting in crater (Su et al., 2006; Oliaei & Karpat, 2016; Arrazola et al., 2009; Davim, 2014), Titanium's limited heat conductivity raises temperatures at the rake face and cutting edge (Armendia et al., 2010; Ribeiro et al., 2003; Ezugwu et al., 2003; Liu et al., 2020; Hassanpour et al., 2016); segmented form of the chips causes cyclic pressures, which causes cutting edge surface fatigue (Pramanik, 2014).

Boujelbene (2018) has experimentally studied the influence of different feed rate from 0.1 to 0.2 mm/rev. and cutting speeds in the range of 50 to 250 m/min on localized shearing and tangential cutting force during orthogonal turning of Titanium alloys. Keblouti et al. (2017) experimentally examined the influence of coating material and machining parameters on the performances of cutting tools. A prediction model was developed by Sahoo et al. (2015) using response surface methodology and artificial neural network during machining of AISI 1040 steel under dry environment and optimized the process parameters using surface plot. Nguyen (2020) used heat transfer equations to determine temperature distribution in the workpiece, cutting tool, and chip and a numerical model was developed for temperature distribution in PCBN cutting. Experiment and Numerical studies were conducted by Sahib and Nassrullah (2020) to investigate the effect of feed rate and cutting speed and uncoated and coated tools, in temperature distribution at cutting zone during turning process for steel AISI 1010. Miroslav Lučić et al. (2020) simulated thermodynamic processes of machining and calculated the temperature fields on

* Corresponding author. Tel.: +91-7293889900 Fax.: +91 (422) 2686 274
E-mail addresses: r_ajith@cb.amrita.edu (A. Ramesh)

ISSN 2291-8752 (Online) - ISSN 2291-8744 (Print)

doi: 10.5267/j.esm.2022.11.002

the wedge of the cutting tool. Irfan et al. (2019) optimized machining parameters, during the CNC turning of EN-45 spring steel, of depth of cut, feed rate, and cutting speed. Surface roughness and MRR were considered as the responses in this work which used Taguchi method and regression analysis as the optimization methods.

Korkmaz and Yasar (2021) numerically examined the effect of cutting parameters on the shear angles, chip morphology, and chip thickness during turning of AA6061-T6 alloys. Jaiswal et al. (2020) developed a numerical model using Abaqus® explicit 6.14 software and is validated using experiments conducted during turning operation on heat-treated Titanium alloy. Javidikia (2020) numerically studied the influence of cutting conditions and tool geometry on chip thickness, machining forces, and cutting temperature during machining of Al 6061-T6. Sadeghifar et al. (2018b) optimized and identified optimal machining parameters to improve machinability and residual stresses produced by orthogonal turning 300M steel. Sadeghifar et al. (2018a) numerically predicted the machining characteristics including surface integrity characteristics including microstructural changes and residual stresses, cutting forces, tool wear, cutting temperature, chip morphology, and burr formation. Mir et al. (2018) experimentally and numerically studied the influence of tool rake angle in single point diamond turning of silicon. DNVPO et al. (2019) researched the residual stresses caused by milling in AISI 1045 steel. Statistical approaches were also used to determine the influence of the cutting parameters. By reducing the real part of the frequency response function, which measures how a cutting tool responds to a harmonic force, Saravanamurugan et al. (2021) optimised cutting tool shape and cutting parameters of the turning process.

Zhuang et al. (2018) established an analytical model to predict the cutting forces during oblique turning. Zhou et al. (2019) studied the effect of cutting parameters on temperature, cutting force and residual stress. Asad et al. (2019) examined and optimized the effect of feed rate, and cutting speed, and tool rake angles on burr lengths. Optimization was done using Taguchi and RSM. Prakash et al. (2020) optimized material and cutting parameters for surface finish and Material Removal Rate (MRR) using Taguchi and Grey Relational Analysis (GRA). Sahu et al. (2019) used TLBO, JAYA and GA optimization strategies for the combined decrease of machined cutting forces and surface roughness in Ti-6Al-4V turning. Li et al. (2020) obtained the optimal machining condition under multi-objective optimization of surface roughness and cutting force using RSM and ITLBO. Çelik et al. (2017) analysed the effect of machining parameters (feed rate, cutting speed, cutting length, and depth of cut) on tool wear and surface roughness during dry turning of Ti-6Al-4V alloy. Rao (2019) optimized the process parameters in orthogonal turn milling of Silicon Bronze using TLBO technique.

From the above literature review, it was understood that there are not enough literatures available on the comparison of available optimization techniques over optimization of orthogonal turning of Ti6Al4V alloys. In the available literature, either RSM and Taguchi or RSM and TLBO are compared. The main objective of this work is to compare the different optimization techniques (RSM, Taguchi, TLBO) applicable to the present work. In this work Ti6Al4V alloys are used as the workpiece material. Orthogonal turning experiments are conducted on the material for a certain combination of machining parameters – Depth of Cut, Feed Rate, and Cutting Speed after selecting speeds in the range of High-Speed Machining. Cutting Forces from the experiments are noted using a Lathe Tool Dynamometer. Using the experimental results, the developed model is validated. Optimization of machining parameters for minimum Cutting Force was performed using three different techniques, namely RSM, Taguchi, and TLBO. The best combination of machining parameters and the optimal Cutting Force value from techniques are compared. Also, the effect of cutting parameters on Cutting Force is investigated in detail using Analysis of Variance (ANOVA).

2. Experiment Details

2.1 Work piece material

Grade 5 Titanium alloy (Ti-6Al-4V) was the workpiece material used to conduct experiments. Cylindrical Specimens having 35 mm dia. and 60 mm long were used. **Table 1** shows the chemical composition of Ti-6Al-4V alloy and the important mechanical and thermal properties are given in **Table 2**.

Table 1. % Composition and mechanical properties of Ti alloy. (Ali 2013)

Constituents	Ti	C	Fe	N	Al	V	H
Composition	89.29	0.05	0.09	0.01	6.15	4.40	0.005

Table 2. Mechanical and Thermal properties of Ti alloy (Ali 2013)

Mechanical		
Density 4428 Kg/m^3	Young's Modulus 113.8 GPa	Poisson's Ratio 0.342
Thermal		
Conductivity 7.4 W/mK	Specific heat 611 W/m^{2}K	Coe. of linear expansion 8.6E-6 /^{0}C

2.2 Cutting tool material

Coated carbide tool inserts of Kennametal make, are used in the turning of titanium alloys. Coated titanium nitrate TiN inserts, along with the tool holder PSBNR2525M12 (Tool geometry: clearance angle = 6^0, rake angle = 0^0) were used in this investigation.

2.3 Experimental Details

Dry orthogonal turning experiments were performed using a conventional lathe with 2.2 kW spindle power. The cutting forces, feed force, radial force, and tangential force, generated while machining is measured with the help of lathe tool dynamometer. Details of the data are given in Ramesh et al. (2015). In the current work, Depth of Cut (DoC), Feed Rate (FR), and Cutting Speed (CS) have been considered as machining parameters. The factors and their associated levels are given in Table 3. These values are selected in such a way that all the machining operations will fall under the High-Speed Machining category. Experiments were performed on a certain combination of machining factors and the cutting forces are recorded and shown in **Table 4**.

Table 3. Cutting Parameters and their levels

Parameters	L1	L2	L3
CS (rpm)	580	690	800
FR (mm/revn.)	0.25	0.35	0.45
DoC (mm)	0.1	0.15	0.2

Table 4. Cutting forces obtained from experiments.

CS (rpm)	FR (mm/rev.)	DoC (mm)	Cutting Force (N)
800	0.25	0.2	70.08
800	0.35	0.2	74.87
800	0.45	0.2	78.63
580	0.25	0.2	70.34

3. Analytical Models for Orthogonal Cutting

Analytical models are relations connecting machining forces and cutting conditions based on the type of cutting. These models are simple to use, however they do necessitate prior knowledge of shear, medium friction, and chip angles (Chen et al., 2015). The use and accuracy of these models are limited because these values must be obtained experimentally.

(i) Ernst & Merchant Model – Assumptions in this model are that the chip is considered as a rigid body, the chip is under the influence of forces from the rake face of tool and shear surface. Based on these assumptions the developed equation for shear angle is given by Eq, (1) (Shaw, 2005).

$$\emptyset = \frac{1}{2}\left(\frac{\pi}{2} + \alpha - \gamma\right) \tag{1}$$

where α is the rake angle of the tool and γ is the friction angle. But this model is considered oversimplified and does not include the effect of work hardening, strain, and strain rates during machining.

(ii) Lee & Shaffer Model – In this model a slip line was used to model chip formation. The material in front of the tool acts as ideal plastic, and there is no hardening in the chip. The slip line field was triangular in shape and situated next to the tool's cutting edge. Based on these assumptions, the obtained equation for shear angle is given by Eq. (2) (Shaw, 2005). Work hardening, inertial effects, and heat effects during machining were not included in this model.

$$\emptyset = \frac{1}{2}\left(\frac{\pi}{2} + 2\alpha - 2\gamma\right) \tag{2}$$

(iii) Oxley's Model – This model introduces the use of parallel sided shear zone model to analyse orthogonal turning. This model assumes primary shear zone thickness was a tenth of the length of the shear zone and plastic flow pattern occurred in this zone. Based on these assumptions, the derived expression for shear angle is given by Eq. (3) (Shaw, 2005). The main drawback of this model is that it requires stress – strain data at different temperatures and strain rates during machining.

$$\emptyset = 50^0 - 0.8(\gamma - \alpha) \tag{3}$$

Using the above three equations the shear angle was calculated using the cutting condition (Cutting Speed = 800 rpm = 1465.33 mm/s = 87.92 m/min, Feed Rate = 0.25 mm/revn, Depth of Cut = 0.2 mm). Then using Eq. (4) (Shaw, 2005), the corresponding cutting force was calculated and comparison with experimental cutting force is shown in Table 5. The error variations may be due to the assumptions used in the models.

$$F_c = \frac{\mathrm{tbK}\cos(\beta - \alpha)}{\sin\emptyset\cos(\emptyset + \beta - \alpha)} \tag{4}$$

where t is the feed rate in mm/revn., b is the depth of cut in mm, and K is the Shear Strength of the material which is taken as 760 MPa (Ran & Chen 2018).

Table 5. Comparison of Cutting Force from Analytical Models with Experiment

	Ernst & Merchant Model	Lee & Shaffer Theory	Oxley's Theory	From Experiments
Cutting Force (N)	83.23	81.25	79.41	70.08
% Error	18.76	15.94	13.31	

Analytical approaches have severe limitations if they are to be applied to practical machining operations involving three dimensional effects and non-steady cutting conditions. The strain hardening of the workpiece material is not taken into account in the analytical models provided in the literature. Furthermore, temperature increases in the deformation zones as a result of plastic deformation and friction, resulting in material softening, are not considered. This means that any good model of the metal cutting process must be able to deal with a coupled mechanical and heat transfer problem. Such combined analysis can be performed using the finite element technique (FEM). The FEM produces results that are extremely near to real-world values, and as a result, it is currently a widely used numerical method. (Kohir, 2014).

4. Numerical Modelling of Orthogonal Turning Process

Because of advances in computational efficiency and speed, finite element techniques (FEM) have become widely used in academic and industry applications in recent years. When compared to analytical models, FEM-based simulations have numerous advantages. Finite element cutting simulations can estimate process variables that are difficult or impossible to measure directly during the cutting process, such as effective stress, normal stress, temperature of chip, tool temperature, strain rate and strain. These parameters must be determined in order to understand the mechanics of the cutting process and undertake tool wear analysis (Kohir, 2014; Hribersek et al., 2018; Narayanan et al., 2020; Jagadeesh & Samuel, 2015; Shi & Attia, 2010; Outeiro et al., 2015; Yaich et al., 2020). The numerical model is developed using ABAQUS/Explicit in this study. In order to estimate the impacts of machining parameters on the cutting force while the turning process of TI6Al4V alloy, a 2D numerical model (**Fig. 1**) is first created. The workpiece is designed to be deformable, and the tool is designed to be analytically rigid. The tool's rake angle and clearance angle are assumed to be 0^0 and 6^0 degrees, respectively. The JC material model parameter for Ti6Al4V alloy used in this work is given in **Table 6**.

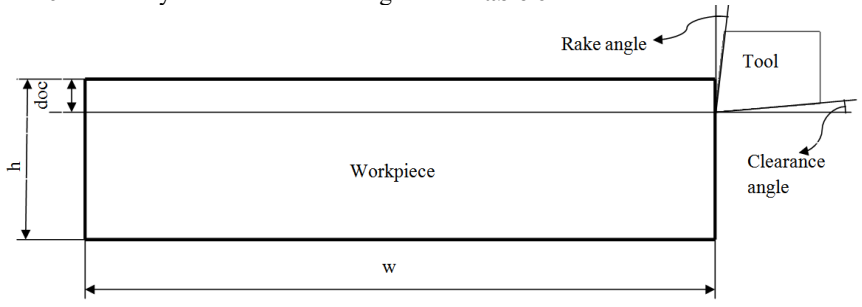

Fig. 1. The geometry of 2D orthogonal cutting

The model assumes that the plastic strain at the start of damage is a function of stress triaxiality and strain rate (Smith, 2009). The JC damage model parameters for Ti6Al4V alloy used in this work is given in **Table 6.**

Table 6. JC Material Model (Kay 2002) and Damage Model Parameters (Johnson & Cook 1985)

A MPa	B Mpa	C	N	m	Tr (^{0}C)	Tm (^{0}C)	$\dot{\varepsilon}_0$	D_1	D_2	D_3	D_4	D_5
1098	1092	0.014	0.93	1.1	25	1680	10^{-5}	-0.09	0.25	-0.5	0.014	3.87

Initially a mesh convergence study is conducted. Surface to surface interaction is employed in this investigation, with a constant friction coefficient of 0.24. The workpiece's lower and left edges are both subjected to an encastre boundary condition. As the boundary condition, a determined velocity value is applied to the reference point on the tool in the negative x-direction. The tool's vertical displacement and in-plane rotation are also restricted. CPE4RT elements of the plane strain element type are employed in the model. The fracture energy, which is used to quantify the material deterioration that occurs once damage occurs in a workpiece, is changed in this study until the simulation results show a satisfactory agreement with the experimental results under the given cutting conditions (refer **Table 4**). In detail, on the given mesh condition, the initial value for fracture energy is estimated by;

$$G_f = \left(\frac{1-\vartheta^2}{E}\right) {K_{Ic}}^2 \tag{5}$$

where $K_{I}c$ is the material's fracture toughness, which is equivalent to 45MPa$\sqrt{}$m (Chen et.al 2011). To retain the same energy density, the failure energy Gf should be adjusted for various cutting situations., as shown in Eq. 6, depending on the ratio of different characteristic lengths L1, L2.

$$\frac{G_{f1}}{G_{f2}} = \frac{doc1}{doc2} = \frac{h1}{h2} = \frac{w1}{w2} = \frac{L1}{L2} \tag{6}$$

Simulations are carried out for combinations of machining parameters shown in **Table 4** and validated the FE model results by comparing the values with experimental results and shown in **Fig. 2.** The maximum deviation is found to be 2.54%.

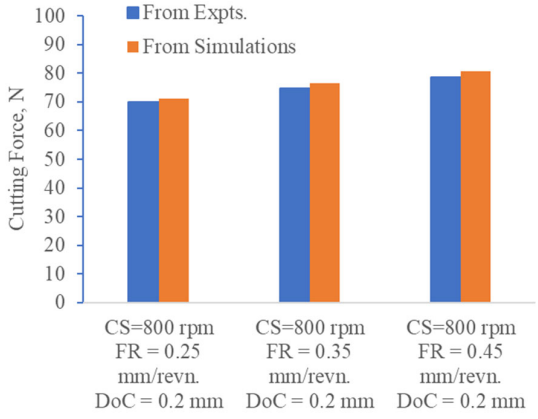

Fig. 2. Validation of Numerical model with Experimental Results

In the validated model, by changing the tool and workpiece geometry and modifying the fracture energy value based on Eq. (6), simulations are run for all combinations obtained from Minitab for different optimization techniques. Cutting forces are measured as reaction forces at the reference point on the tool.

5. Optimization Techniques (RSM, Taguchi & TLBO)

5.1 Introduction to Response Surface Methodology (RSM)

The impact of machining parameters on cutting force was investigated using the DoE programme Minitab 18. To identify the number of trials to be considered for the optimization of variables, central composite design technique is utilized. A typical central composite design, named Face Centered Design is used in this analysis (Aydar, 2018; Palanikumar et al., 2008). Based on these, 20 trials were generated, and simulations are run in the validated model for each trial. The 20 trials and the cutting force noted in each trial are shown in **Table 7** below.

Table 7. 20 RSM Trails and Cutting Force

Trial No.	CS (rpm)	FR (mm/revn.)	DoC (mm)	Fc (N)
1	580	0.35	0.15	74.85
2	800	0.25	0.2	71.17
3	690	0.35	0.15	70.93
4	690	0.35	0.15	70.93
5	800	0.45	0.1	70.31
6	580	0.45	0.2	78.87
7	800	0.35	0.15	69.32
8	580	0.25	0.2	70.34
9	580	0.25	0.1	60.01
10	690	0.45	0.15	74.48
11	800	0.25	0.1	62.83
12	690	0.35	0.15	70.93
13	690	0.35	0.15	70.93
14	690	0.25	0.15	67.73
15	690	0.35	0.2	74.53
16	800	0.45	0.2	80.63
17	690	0.35	0.15	70.93
18	580	0.45	0.1	71.12
19	690	0.35	0.15	70.93
20	690	0.35	0.1	67.73

ANOVA is performed for the cutting force values and the Rsqu. value is noted. This value shows how the better the model fits your data. In the ANOVA confidence interval of 5% is used. So, the terms having P-value greater than 0.05 are considered as non-significant terms and are removed from the ANOVA. Further, ANOVA is performed again with significant terms and the regression equation of response surface obtained. Main effect plot is plotted to identify the influence of machining

parameters on cutting force. Using the response optimizer option available in the software, the optimum combination of machining parameters is identified.

5.2 Introduction to Taguchi

Taguchi explains how to use experimental design to design products/processes that are resistant to environmental conditions, as well as to design and develop products/processes that are resistant to component variation, and to minimise variation around a target value. The Taguchi approach to design of experiments (DOE) has a high widespread adoption, allowing users to apply it with only a basic understanding of statistics. As a result, it has received significant use in engineering applications (Peksen & Kalyon, 2021). Numerous tests must be performed as the number of process parameters increases. The Taguchi technique solves this problem by studying the whole parameter space with a minimal number of experiments using a particular design of orthogonal arrays. The difference between the experimental and intended values is then calculated using a loss function. The S/N ratio is computed for each level of process parameters based on the S/N analysis. In addition, an analysis of variance (ANOVA) is used to determine whether process factors are statistically significant. If the goal is to limit variability around a certain target, nominal the best is utilised; lower the better if the system is optimised for the largest possible reaction, and larger the better if the system is optimised for the smallest possible response. The optimal factor levels are those that optimise the proper S/N ratio. The requirement of this work was to discover the optimal combination of machining settings for reducing Cutting Force. In this investigation, a smaller-the-better quality feature was used since lower Cutting Force reflects better or enhanced surface condition and tool life. An orthogonal array specifies the number of trials required to determine the best suited factors for use in the manufacturing or design of a product (Murthy et al., 2017). In this work L27 OA is used to find the best combination of cutting parameters which minimises the cutting force. Table 8 shows the different combination of machining parameters based on this array using Minitab18. Simulations were carried out for each of these trails in the validated FE model and the corresponding cutting forces are noted and shown in **Table 8**.

Table 8. 27 Taguchi Trails and Cutting Force

Trial No.	CS (rpm)	FR (mm/revn.)	DoC (mm)	Fc (N)	S/N Ratio
1	580	0.25	0.1	60.01	-35.5645
2	580	0.25	0.15	71.13	-37.0411
3	580	0.25	0.2	68.93	-36.944
4	580	0.35	0.1	63.31	-36.0294
5	580	0.35	0.15	74.85	-37.4838
6	580	0.35	0.2	66.67	-36.4786
7	580	0.45	0.1	71.12	-37.0398
8	580	0.45	0.15	77.62	-37.7995
9	580	0.45	0.2	78.87	-37.9382
10	690	0.25	0.1	59.63	-35.5093
11	690	0.25	0.15	67.33	-36.5642
12	690	0.25	0.2	69.23	-36.8059
13	690	0.35	0.1	67.73	-36.6156
14	690	0.35	0.15	70.93	-37.0166
15	690	0.35	0.2	74.53	-37.4466
16	690	0.45	0.1	70.08	-36.9119
17	690	0.45	0.15	74.48	-37.4408
18	690	0.45	0.2	76.87	-37.7151
19	800	0.25	0.1	66.83	-36.4994
20	800	0.25	0.15	66.68	-36.4799
21	800	0.25	0.2	71.17	-37.0459
22	800	0.35	0.1	66.52	-36.459
23	800	0.35	0.15	69.32	-36.8172
24	800	0.35	0.2	76.63	-37.251
25	800	0.45	0.1	70.31	-36.9403
26	800	0.45	0.15	73.38	-37.3116
27	800	0.45	0.2	80.63	-38.0215

5.3 Introduction to Teaching Learning Based Optimization (TLBO)

TLBO approach is based on the impact of a teacher's influence on the production of students in a classroom. The algorithm simulates a teacher's and students' capacity to teach and learn in a classroom. The method is depicted in a flow chart (Sahu & Andhare2015). The algorithm explains two primary forms of learning: learning through a teacher (known as the teacher phase) and learning by engaging with other learners (known as the learner phase). Furthermore, learners benefit from their interactions with one another, which helps them improve their performance. The population size (values of feed, cutting speed, and depth of cut within a specific range) is examined in this method, and design variables (such as feed, cutting speed, and depth of cut) are considered as distinct subjects offered to learners. TLBO code was generated using MATLAB R2017a.

6. Results and Discussions

6.1 Analysis of Variance for Cutting Force using RSM

In this work, DoE software Minitab 18 was used to analyse the influence of machining parameters on cutting force. The central composite design method is used to determine the number of experiments to be evaluated for the optimization of the variables and responses. A typical central composite design, named Face Centered Design is used in this analysis. Based on these, 20 trials were generated, and simulations were run in the validated model for each trial. The 20 trials and the cutting force noted in each trial are shown in **Table 7**. ANOVA was performed for the cutting force values and the R squ. value was found to be 92.78%, which is close to a cent percent. This shows how the better the model fits your data. It was found that the square term of depth of cut and interaction between cutting speed & feed rate and interaction between feed rate & depth of cut are insignificant terms. Hence, these terms are removed, and ANOVA is performed again. The regression equation obtained for cutting force is given in Eq. (7).

$$\mathrm{Fc} = 43.33 - 0.00085 * \mathrm{CS} + 43.33 * \mathrm{FR} + 87.08 * \mathrm{DoC} + 0.000001 * \mathrm{CS} * \mathrm{CS} - 0.00001 * \mathrm{FR} * \mathrm{FR} + 0.00001 * \mathrm{CS} * \mathrm{DoC} \quad (7)$$

6.1.1 Influence of machining parameters on Cutting Force

The fluctuation of cutting force with machining parameters is shown in **Fig. 3**. According to this diagram, the feed rate and depth of cut have a considerable impact on cutting force. Cutting speed has a less impact on cutting force, possibly because increasing speed does not result in a large temperature change in the quickly moving primary shear zone. When it comes to feed rate and depth of cut, more material comes into contact with the tool in a given amount of time. As a result, it takes greater force to remove the material (Sumesh & Ramesh, 2018).

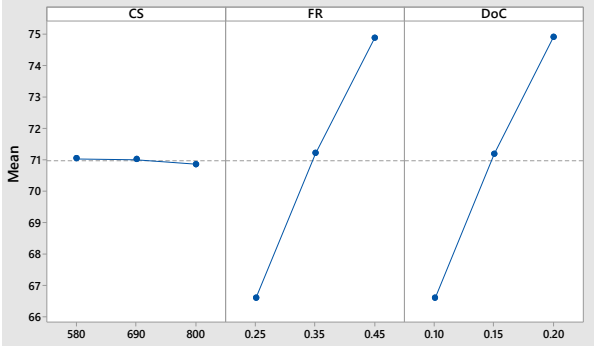

Fig. 3. Variation of Cutting Force with Machining Parameters

Fig. 3(a)-(c) show variation of cutting force with two machining parameters in 2D and 6(d)-(f) represent the variation of cutting force with two parameters at a time in 3D plot. In these figures, the same trend observed in **Fig. 3** can be noticed.

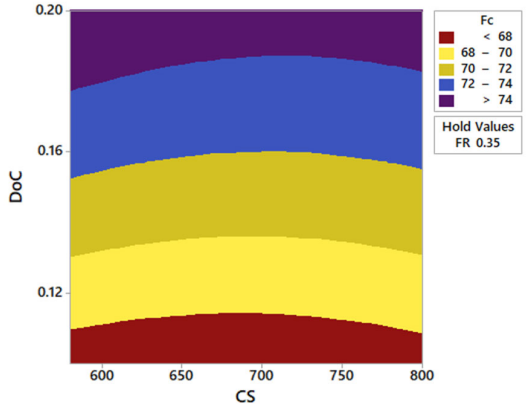

(a)

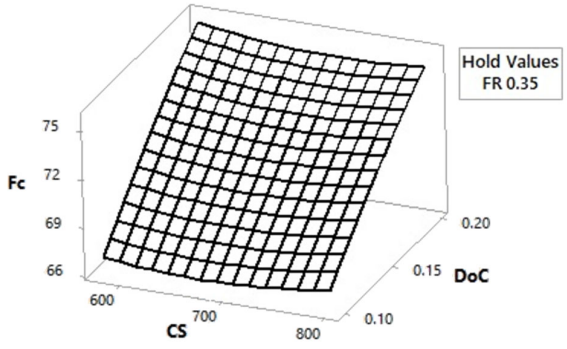

(d)

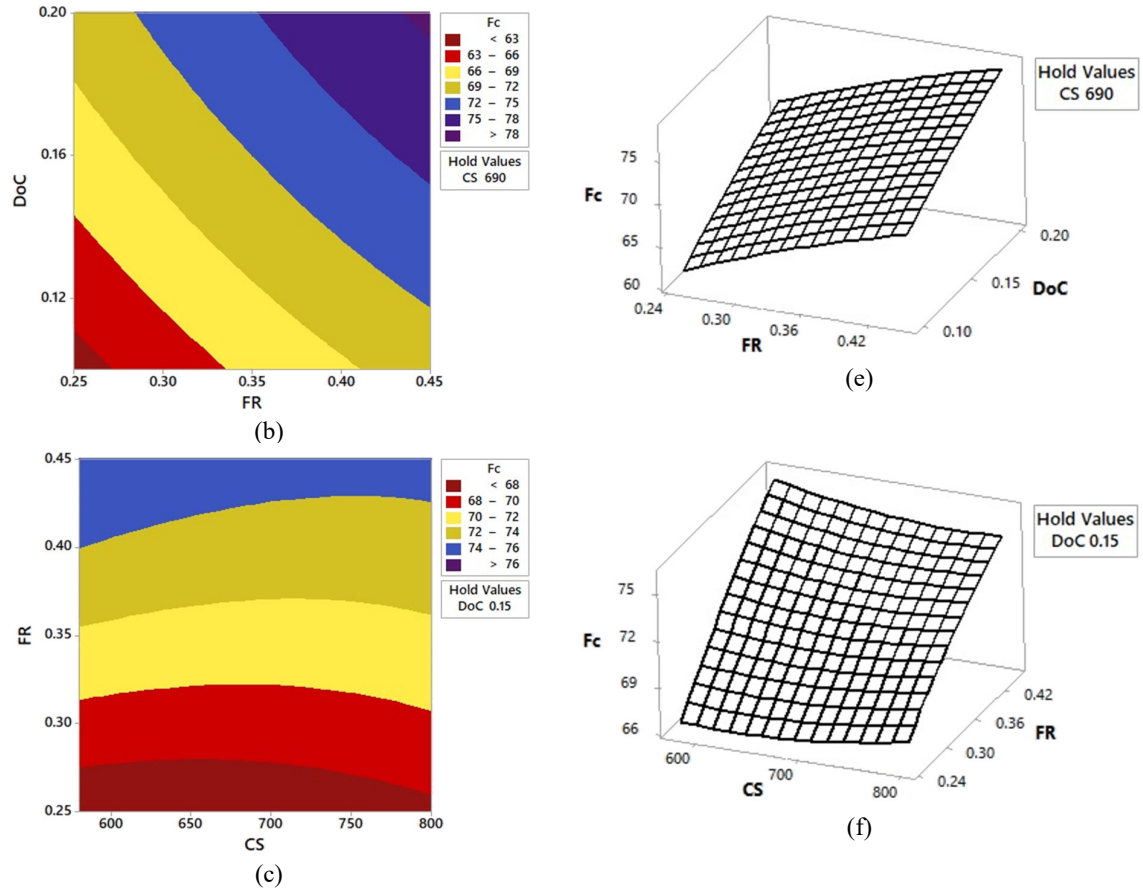

Fig. 3. Variations of Cutting Force with Machining Parameters

Using the desirability function, the optimal combination of machining parameters was identified. The desirability value is D = 0.9287 and the optimized machining parameters are CS = 671.1 rpm, FR = 0.25 mm/rev. and DoC = 0.1 mm. The corresponding cutting force is 61.48 N.

6.2 Optimization of Machining Parameters using Taguchi Method

Since it is selected as lower magnitude of Cutting Force (Fc) is the better type quality characteristic, from **Fig. 5**, it can be seen that the second level of cutting speed (A2) = 690 rpm, first level of feed rate (B1) = 0.25 mm/rev, and first level of depth of cut (C1) = 0.10 mm results in minimum value of Cutting Force. It is observed from **Fig. 5** that Fc is almost constant with an increase in cutting speed, but with a decreasing trend. The Fc is continuously decreased with increase in feed rate and for depth of cut.

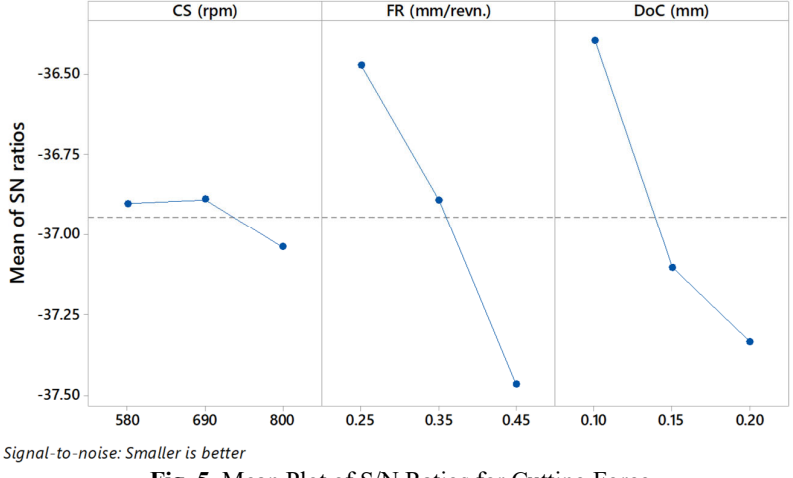

Fig. 5. Mean Plot of S/N Ratios for Cutting Force

From the ANOVA analysis for Cutting Force using Taguchi, after calculating percentage contribution for all control factors, it is found from the Tables 9 and 10, feed rate and depth of cut are the most significant control factors for cutting force.

Table 9. Response Table for Signal to Noise Ratios

Level	CS (rpm)	FR (mm/revn.)	DoC (mm)
1	-36.90	-36.84	-36.40
2	-36.89	-36.89	-37.11
3	-37.04	-37.47	-37.34
Delta	0.15	0.99	0.94
Rank	3	1	2

Table 10. Response Table for Means

Level	CS (rpm)	FR (mm/revn.)	DoC (mm)
1	70.28	66.77	66.17
2	70.09	70.05	71.75
3	71.27	74.82	73.73
Delta	1.18	8.05	7.55
Rank	3	1	2

The optimum combination of machining parameters obtained are Cutting Speed = 690 rpm, Feed rate = 0.25 mm/revn., and Depth of cut = 0.1 mm. and the corresponding Cutting Force obtained is 60.88 N.

6.3 Optimization of Machining Parameters using TLBO

The major aim of this work is to find the best machining parameters for reducing cutting force. The turning process was written in a conventional optimization problem format that could be addressed with a numerical optimization technique for this purpose. Standard optimization problem definitions call for the minimization of an objective function and the satisfaction of constraint functions in terms of optimization parameters (Sahu & Andhare 2015).
The optimization challenge for Ti-6Al-4V machining is as follows:

$$\text{Objective } Z = \text{Min Fc (CS, FR, DoC)} \tag{8}$$

During the optimization process, the ranges of allowable modifications in the input parameters are:

$$\begin{aligned} CS_{min} \leq CS \leq CS_{max} \\ FR_{min} \leq FR \leq FR_{max} \\ DoC_{min} \leq DoC \leq Doc_{max} \end{aligned} \tag{9}$$

Table 3 shows the low, middle, and high values for the variables. The objective function is the expected model for cutting force developed using RSM, i.e. Eq. (7). The problem is then solved using the Teaching Learning Based Algorithm (TLBO). The TLBO code, written in MATLAB code and used for the optimization of cutting force. This approach is repeated until the best solution is consistently reached by repeating Teacher Phase and Learner Phase. The optimal combination of Cutting parameters produced by the TLBO method is cutting speed = 580 rpm, feed rate = 0.25 mm/revn., and depth of cut = 0.1 mm and the corresponding Cutting Force obtained is 62.38 N.

6.4 Comparison of Optimized Values of Cutting Force

Table 11 shows the comparison of three optimization techniques, namely RSM, Taguchi, and TLBO. It can be found that feed rate and depth of cut values obtained from three techniques are the same and the cutting speed values are different. Also, the cutting force value predicted by all the three methods are almost same.

Table 11. Comparison of RSM, Taguchi, and TLBO Results

Sl. No.	Optimization Technique	CS (RPM)	FR (mm/revn.)	DoC (mm)	Cutting Force (N)
1	Using RSM	671.1	0.25	0.1	61.48
2	Using Taguchi	690	0.25	0.1	60.88
3	Using TLBO	580	0.25	0.1	62.38

Confirmation tests were carried out at CS = 690 rpm, FR = 0.25 mm/revn., and DoC = 0.1 mm combination of machining parameters in the validated numerical model, which produces minimum cutting force of 60.88 N, and the results are shown in Table 12 below. It was found that, the error variation of cutting force obtained from the finite element model with the experiments is less than 2%. This means that the developed model can be used to find the cutting force for any combination of machining parameters effectively.

Table 12. Confirmation Test Results

Machining Combination	Cutting Force, N		
	From optimization	From Experiment	From Simulation
CS = 690rpm FR = 0.25 mm/revn. DoC = 0.1 mm	60.88	58.86	59.63

7. Conclusions

The present work aims at comparison of available optimization techniques, RSM Taguchi and TLBO for the Orthogonal Turning processes. Experiments were conducted for different values of Cutting Speed, Feed rate and Depth of cut and measured the cutting force. Some popular analytical models such as Merchant's, Lee & Shaffer and Oxley's were considered for modeling the orthogonal turning process. But due to the disadvantages of the analytical models, further studies were carried out using FEM. A numerical model was developed to simulate the orthogonal turning process and the same is validated with experimental results. To compare and find the optimal machining parameter combination, initially RSM was used for optimization and to investigate the effect of machining parameters. Further, another optimization technique Taguchi was used for the analysis. Next, advanced algorithm TLBO was used to find the optimal machining parameter combination. The results obtained from the three techniques were compared. The main conclusions from this study are:

1. Analytical models such as Ernst & Merchant, Lee & Shaffer and Oxley's were considered in this study. The Cutting Force values obtained from these models are compared with Experimental values. The error percentage found was high. It may be due to non- consideration of stain, strain rates and temperature during machining, in the models.
2. Developed numerical model is validated with experiments conducted and it was found that the model can be used for effective prediction of the cutting force.
3. In general, it was found that cutting speed has less influence than feed rate and depth of cut on cutting force (Fc) value. Thus, lower values of feed rate and depth of cut will produce minimum cutting force.
4. From the RSM results on influence of machining parameters on cutting force, it was obtained that the feed rate and depth of cut have significant influence on cutting force. Also, it was observed that cutting speed has less influence on cutting force. Increase in cutting speed increases temperature in the primary shear zone, which softens the material and thereby reduces the cutting force. When the feed rate and depth of cut increases, more material comes in contact with the cutting tool, which increases the cutting force. Minimum cutting force happens at low values of feed rate and depth of cut.
5. From the Taguchi Optimization results, it was observed that low values of depth of cut and feed rate second level of cutting speed will produce minimum cutting force. Also, it was found that, feed rate and depth of cut are the significant parameters for minimum cutting force.
6. Based on the comparison of different optimization techniques like RSM, Taguchi, TLBO, it was found that all models can be used successfully to predict cutting force during orthogonal turning of Ti6Al4V alloys.
7. Confirmation simulations were ran on the validated model and found that results are well acceptable, and the variations are within less than 2% only. This means that the developed model can be used to predict cutting force during orthogonal turning of Ti6Al4V alloys accurately.

References

Ali, M. H., Khidhir, B. A., Ansari, M. N. M., & Mohamed, B. (2013). FEM to predict the effect of feed rate on surface roughness with cutting force during face milling of titanium alloy. *Hbrc Journal, 9*(3), 263-269.

Armendia, M., Garay, A., Iriarte, L. M., & Arrazola, P. J. (2010). Comparison of the machinabilities of Ti6Al4V and TIMETAL® 54M using uncoated WC–Co tools. *Journal of Materials Processing Technology, 210*(2), 197-203.

Arrazola, P. J., Garay, A., Iriarte, L. M., Armendia, M., Marya, S., & Le Maître, F. (2009). Machinability of titanium alloys (Ti6Al4V and Ti555. 3). *Journal of materials processing technology, 209*(5), 2223-2230.

Asad, M., Ijaz, H., Saleem, W., Mahfouz, A. S., Ahmad, Z., & Mabrouki, T. (2019). Finite element analysis and statistical optimization of end-burr in turning AA2024. *Metals, 9*(3), 276.

Aydar, A. Y. (2018). Utilization of response surface methodology in optimization of extraction of plant materials. *Statistical approaches with emphasis on design of experiments applied to chemical processes*, 157-169.

Bandapalli, C., Singh, K. K., Sutaria, B. M., & Bhatt, D. V. (2018). Experimental investigation of top burr formation in high-speed micro-end milling of titanium alloy. *Machining Science and Technology, 22*(6), 989-1011.

Boujelbene, M. (2018). Investigation and modeling of the tangential cutting force of the Titanium alloy Ti-6Al-4V in the orthogonal turning process. *Procedia manufacturing, 20*, 571-577.

Çelik, Y. H., Kilickap, E., & Güney, M. (2017). Investigation of cutting parameters affecting on tool wear and surface roughness in dry turning of Ti-6Al-4V using CVD and PVD coated tools. *Journal of the Brazilian Society of Mechanical Sciences and Engineering, 39*(6), 2085-2093.

Chen, G., Ren, C., Yang, X., Jin, X., & Guo, T. (2011). Finite element simulation of high-speed machining of titanium alloy (Ti–6Al–4V) based on ductile failure model. *The International Journal of Advanced Manufacturing Technology, 56*(9), 1027-1038.

Chen, Y., Li, H., & Wang, J. (2015). Further development of Oxley's predictive force model for orthogonal cutting. *Machining Science and Technology, 19*(1), 86-111.

Choudhary, A., & Paul, S. (2019). Performance evaluation of PVD TIALN coated carbide tools vis-à-vis uncoated carbide tool in turning of titanium alloy (Ti-6Al-4V) by simultaneous minimization of cutting energy, dimensional deviation and tool wear. *Machining Science and Technology, 23*(3), 368-384.

D N V, P. O., Marimuthu K, P., & M, T. (2019). Effect of Speed, Feed and Depth of Cut on Machining Induced Residual Stresses in Aisi 1045 Steel. In International Journal of Recent Technology and Engineering (IJRTE) (Vol. 8, Issue 2, pp. 3397–3400). Blue Eyes Intelligence Engineering and Sciences Engineering and Sciences Publication - BEIESP. https://doi.org/10.35940/ijrte.a1262.078219

Davim, J. P. (2014). *Machining of Titanium Alloys*. Springer. https://doi.org/10.1007/978-3-662-43902-9

Ezugwu, E. O., Bonney, J., & Yamane, Y. (2003). An overview of the machinability of aeroengine alloys. *Journal of materials processing technology, 134*(2), 233-253.

Gao, C., & Zhang, L. (2013). Effect of cutting conditions on the serrated chip formation in high-speed cutting. *Machining Science and Technology, 17*(1), 26-40.

Hassanpour, H., Sadeghi, M. H., Rezaei, H., & Rasti, A. (2016). Experimental study of cutting force, microhardness, surface roughness, and burr size on micromilling of Ti6Al4V in minimum quantity lubrication. *Materials and Manufacturing Processes, 31*(13), 1654-1662.

Hribersek, M., Pusavec, F., Rech, J., & Kopac, J. (2018). Modeling of machined surface characteristics in cryogenic orthogonal turning of inconel 718. *Machining Science and Technology, 22*(5), 829-850.

Jagadesh, T., & Samuel, G. L. (2015). Mechanistic and finite element model for prediction of cutting forces during micro-turning of titanium alloy. *Machining Science and Technology, 19*(4), 593-629.

Jaiswal, A. P., Khanna, N., & Bajpai, V. (2020). Orthogonal machining of Heat Treated Ti-10-2-3: FE and Experimental. *Materials and Manufacturing Processes, 35*(16), 1822-1831.

Jamil, M., Khan, A. M., He, N., Li, L., Iqbal, A., & Mia, M. (2019). Evaluation of machinability and economic performance in cryogenic-assisted hard turning of α-β titanium: a step towards sustainable manufacturing. *Machining Science and Technology, 23*(6), 1022-1046.

Javidikia, M., Sadeghifar, M., Songmene, V., & Jahazi, M. (2020). On the impacts of tool geometry and cutting conditions in straight turning of aluminum alloys 6061-T6: an experimentally validated numerical study. *The International Journal of Advanced Manufacturing Technology, 106*(9), 4547-4565.

Johnson, G. R., & Cook, W. H. (1985). Fracture characteristics of three metals subjected to various strains, strain rates, temperatures and pressures. *Engineering fracture mechanics, 21*(1), 31-48.

Kay, G. (2002). Failure modeling of titanium-6Al-4V and 2024-T3 aluminum with the Johnson-Cook material model (No. UCRL-ID-149880). Lawrence Livermore National Lab., CA (US).

Keblouti, O., Boulanouar, L., Azizi, M., & Athmane, M. (2017). Modeling and multi-objective optimization of surface roughness and productivity in dry turning of AISI 52100 steel using (TiCN-TiN) coating cermet tools. *International Journal of Industrial Engineering Computations, 8*(1), 71-84.

Kohir, V., & Dundur, S. T. (2014). Finite Element Simulation to study the effect of flank wear land inclination on cutting forces and temperature distribution in orthogonal machining. *Journal of Engineering Fundamentals, 1,* 30-42.

Korkmaz, M. E., & Yaşar, N. (2021). FEM modelling of turning of AA6061-T6: Investigation of chip morphology, chip thickness and shear angle. *Journal of Production Systems and Manufacturing Science, 2*(1), 50-58.

Li, B., Tian, X., & Zhang, M. (2020). Modeling and multi-objective optimization of cutting parameters in the high-speed milling using RSM and improved TLBO algorithm. *The International Journal of Advanced Manufacturing Technology, 111*(7), 2323-2335

Liu, L., Wu, M., Li, L., & Cheng, Y. (2020). FEM simulation and experiment of high-pressure cooling effect on cutting force and machined surface quality during turning Inconel 718. *Integrated Ferroelectrics, 206*(1), 160-172.

Lučić, M., Marušić, V., Baralić, J., & Mitrović, A. (2020). Numerical Analysis of the Temperature Field in the Cutting Zone in Continuous and Discontinuous Metal Cutting by Turning. *Tehnički vjesnik, 27*(5), 1486-1491.

Mir, A., Luo, X., Cheng, K., & Cox, A. (2018). Investigation of influence of tool rake angle in single point diamond turning of silicon. *The International Journal of Advanced Manufacturing Technology, 94*(5), 2343-2355.

Murthy, K. L. N., Sandeep, B., Vanukuru, R., & Chaitanya, T. K. (2017). A Review on Taguchi's Technique of forming Orthogonal Arrays. *Journal of Advances in Mechanical Engineering and Science, 3*(3), 9-14.

Narayanan, S. V., Benjamin D, M., Keshav, R., & Raj, D. S. (2020). A combined numerical and experimental investigation of minimum quantity lubrication applied to end milling of Ti6Al4V alloy. *Machining Science and Technology, 25*(2), 209-236.

Nguyen, D. T. Q. (2020). Prediction of Temperature Distribution in PCBN Cutting Tools in Orthogonal Turning 9XC Hardened Alloy Steels. In Advanced Materials (pp. 131-139). Springer, Cham.

Oliaei, S. N. B., & Karpat, Y. (2016). Investigating the influence of built-up edge on forces and surface roughness in micro scale orthogonal machining of titanium alloy Ti6Al4V. *Journal of Materials Processing Technology, 235*, 28-40.

Olvera, D., de Lacalle, L. N. L., Urbikain, G., Lamikiz, A., Rodal, P., & Zamakona, I. (2012). Hole making using ball helical milling on titanium alloys. *Machining Science and Technology, 16*(2), 173-188.

Outeiro, J. C., Umbrello, D., M'Saoubi, R., & Jawahir, I. S. (2015). Evaluation of present numerical models for predicting metal cutting performance and residual stresses. *Machining Science and Technology, 19*(2), 183-216.

Palanikumar, K., Muthukrishnan, N., & Hariprasad, K. S. (2008). Surface roughness parameters optimization in machining A356/SiC/20p metal matrix composites by PCD tool using response surface methodology and desirability function. *Machining Science and Technology, 12*(4), 529-545.

Pekşen, H., & Kalyon, A. (2021). Optimization and measurement of flank wear and surface roughness via Taguchi based grey relational analysis. *Materials and Manufacturing Processes, 36*(16), 1865-1874.

Prakash, K. S., Gopal, P. M., & Karthik, S. (2020). Multi-objective optimization using Taguchi based grey relational analysis in turning of Rock dust reinforced Aluminum MMC. *Measurement, 157,* 107664.

Pramanik, A. (2014). Problems and solutions in machining of titanium alloys. *The International Journal of Advanced Manufacturing Technology, 70*(5), 919-928.

Ramesh, A., Sumesh, C. S., Abhilash, P. M., & Rakesh, S. (2015). Finite element modelling of orthogonal machining of hard to machine materials. *International Journal of Machining and Machinability of Materials, 17*(6), 543-568.

Ran, C., & Chen, P. (2018). Dynamic shear deformation and failure of Ti-6Al-4V and Ti-5Al-5Mo-5V-1Cr-1Fe alloys. *Materials, 11*(1), 76.

Rao, K. V. (2019). A novel approach for minimization of tool vibration and surface roughness in orthogonal turn milling of silicon bronze alloy. *Silicon, 11*(2), 691-701.

Ribeiro, M. V., Moreira, M. R. V., & Ferreira, J. R. (2003). Optimization of titanium alloy (6Al–4V) machining. *Journal of materials processing technology, 143*, 458-463.

Sadeghifar, M., Sedaghati, R., Jomaa, W., & Songmene, V. (2018a). Finite element analysis and response surface method for robust multi-performance optimization of radial turning of hard 300M steel. *The International Journal of Advanced Manufacturing Technology, 94*(5), 2457-2474.

Sadeghifar, M., Sedaghati, R., Jomaa, W., & Songmene, V. (2018b). A comprehensive review of finite element modeling of orthogonal machining process: chip formation and surface integrity predictions. *The International Journal of Advanced Manufacturing Technology, 96*(9), 3747-3791.

Sahib, B. S., & Nassrullah, K. S. (2020). Experimental and Numerical Investigation of Temperature Distribution in the Cutting Zone with Different Coated Tools in Orthogonal Turning Operations. *In IOP Conference Series: Materials Science and Engineering* (Vol. 671, No. 1, p. 012016). IOP Publishing.

Sahoo, A., Rout, A., & Das, D. (2015). Response surface and artificial neural network prediction model and optimization for surface roughness in machining. *International Journal of Industrial Engineering Computations, 6*(2), 229-240.

Sahu, N. K., & Andhare, A. B. (2015, August). Optimization of surface roughness in turning of Ti-6Al-4V Using Response Surface Methodology and TLBO. In International Design Engineering Technical Conferences and Computers and Information in Engineering Conference (Vol. 57113, p. V004T05A020). American Society of Mechanical Engineers. Pervaiz, S., Rashid, A., Deiab, I., & Nicolescu, M. (2014). Influence of tool materials on machinability of titanium-and nickel-based alloys: a review. *Materials and Manufacturing Processes, 29*(3), 219-252.

Sahu, N. K., & Andhare, A. B. (2019). Multiobjective optimization for improving machinability of Ti-6Al-4V using RSM and advanced algorithms. *Journal of Computational Design and Engineering, 6*(1), 1-12.

Sahu, N. K., Andhare, A. B., & Raju, R. A. (2018). Evaluation of performance of nanofluid using multiwalled carbon nanotubes for machining of Ti–6AL–4V. *Machining science and Technology, 22*(3), 476-492.

Saravanamurugan, S., Sundar, B. S., Pranav, R. S., & Shanmugasundaram, A. (2021). Optimization of cutting tool geometry and machining parameters in turning process. *Materials Today: Proceedings, 38*, 3351-3357.

Shaw, M. C., & Cookson, J. O. (2005). Metal cutting principles (Vol. 2, p. 98). New York: Oxford university press.

Shi, B., & Attia, H. (2010). Current status and future direction in the numerical modeling and simulation of machining processes: a critical literature review. *Machining Science and Technology, 14*(2), 149-188.

Smith, M. (2009). ABAQUS/Standard User's Manual, Version 6.9.

Su, Y., He, N., Li, L., & Li, X. L. (2006). An experimental investigation of effects of cooling/lubrication conditions on tool wear in high-speed end milling of Ti-6Al-4V. *Wear, 261*(7-8), 760-766.

Sumesh, C. S., & Ramesh, A. (2018). Numerical modelling and optimization of dry orthogonal turning of Al6061 T6 alloy. Periodica Polytechnica Mechanical Engineering, 62(3), 196-202. Irfan, S. S., Kumar, M. V., & Rudresha, N. (2019). Optimization of machining parameters in CNC turning of EN45 by Taguchi's orthogonal array experiments. *Materials Today: Proceedings, 18*, 2952-2961.

Wu, H., & Guo, L. (2014). Machinability of titanium alloy TC21 under orthogonal turning process. *Materials and Manufacturing Processes, 29*(11-12), 1441-1445.

Yaich, M., Ayed, Y., Bouaziz, Z., & Germain, G. (2020). A 2D finite element analysis of the effect of numerical parameters on the reliability of Ti6Al4V machining modeling. *Machining Science and Technology, 24*(4), 509-543.

Zhou, Y., Sun, H., Li, A., Lv, M., Xue, C., & Zhao, J. (2019). FEM simulation-based cutting parameters optimization in machining aluminum-silicon piston alloy ZL109 with PCD tool. *Journal of Mechanical Science and Technology, 33*(7), 3457-3465.

Zhuang, K., Weng, J., Zhu, D., & Ding, H. (2018). Analytical modeling and experimental validation of cutting forces considering edge effects and size effects with round chamfered ceramic tools. *Journal of manufacturing science and engineering, 140*(8), 081012.